# Stability of the Default Mode Network estimated from electroencephalogram

Joana Silva
School of Innovation,
Design and Engineering
Mälardalen University
Västerås, Sweden
joana.silva@mdu.se

Elmeri Syrjänen
School of Innovation,
Design and Engineering
Mälardalen University
Västerås, Sweden
elmeri.syrjanen@mdu.se

Elaine Astrand
School of Innovation,
Design and Engineering
Mälardalen University
Västerås, Sweden
ORCID: 0000-0002-3869-279X

Abstract—The Default Mode Network (DMN) is associated with an internal self-referential view of the world, and its intrinsic properties have been linked to different cognitive abilities. While its function and structure has been well characterized through functional magnetic resonance imaging (fMRI), much less is known about its behavior using electroencephalography (EEG). This study examines the stability of EEG-based DMN functional connectivity. We focus on eyes-open resting-state across multiple sessions. Using the debiased weighted Phase Lag Index (dwPLI), we analyzed connectivity patterns in the alpha band across four sessions involving twenty participants. Our results show consistent DMN connectivity patterns both within and across individuals and sessions. This indicates that EEG-derived DMN connectivity is relatively stable over time and across people. Such stability could be relevant for the development of brain-computer interfaces (BCI) for cognitive training that adapt to individual connectivity patterns.

Index Terms—Default mode network (DMN), functional connectivity, EEG, resting-state, BCI

# I. INTRODUCTION

The Default Mode Network (DMN) is one of the most studied resting-state networks, observed in functional MRI (fMRI) activity when subjects are not actively engaged in a task. It is the most active brain network when individuals are mentally at rest and not focused on the external environment [1]. In most cases, the DMN reduces its activation when subjects are focused on tasks that require attention to the outside world, but certain processes like self-referential thinking, mind wandering, recalling memories, and internal mental simulations, can activate the DMN [2], [3]. Anatomically, the DMN includes the medial prefrontal cortex (mPFC), posterior cingulate cortex (PCC), precuneus, and lateral posterior parietal cortex [1], [3], [4]. While its structure and function have been extensively characterized using fMRI, its dynamics when estimated from electroencephalogram (EEG) remain less explored, particularly across multiple sessions and in eyesopen conditions. In fact, to the best of our knowledge, no prior studies have examined the stability of EEG-estimated DMN across sessions.

Understanding how the DMN can be estimated from EEG is especially relevant for brain-computer interface (BCI) and neurofeedback training (NFT), as different metrics on its connectivity could provide real-time information on the subject's

mental state. EEG is preferred here due to its accessibility, portability, and real-time feedback capabilities, as recently demonstrated in a 2024 study on real-time DMN activation [5].

Yet, studies evaluating DMN stability over time using EEG are scarce and report inconsistent findings: some studies that tracked resting-state activity using PET and fMRI, reported DMN stability in healthy older adults over a 8-year follow up period [6]. Another study recorded EEG continuously over multiple days (at least 48 hours) [7] and found consistent DMN-related activity in younger adults across different levels of consciousness. On the other hand, a more recent fMRI study suggests that DMN connectivity may change with aging, even in the healthy brain [8]. These age-dependent differences have been linked to changes in working memory, processing speed, and neural plasticity, all of which can influence the outcomes of cognitive training and neural self-regulation. Moreover, an individual's cognitive state on a given day may affect DMN connectivity, which raises intriguing questions about how day-to-day variability impacts NFT performance. Restingstate functional connectivity activation has been linked to NFT performance [9]–[11], but the question of why some individuals are able to self-regulate their neural activity while others fail (16% to 57%), commonly termed "BCI illiteracy" [12], [13], remains open.

Frequency-specific associations also support the DMN's relevance in EEG: the alpha band (8–13 Hz), for instance, has been positively related to posterior regions of the DMN, including parietal-occipital midline cortex [14], [15], and is known to support long-range communication across resting-state networks [16], [17]. Its prominence in resting-state activity justify the importance of this frequency range [18].

Additionally, EEG-based studies have identified subnets of DMN (or operational modules) that approximate the DMN topography usually seen in fMRI studies [19]. Other work has shown enhanced effective connectivity within DMN regions in individuals with social anxiety disorders compared to healthy controls during rest [20], highlighting the DMN as an interesting target for network-level analysis. However, important questions remain: How stable is EEG-measured DMN connectivity across multiple days? Is this stability region-

specific? The present study addresses these questions by analyzing DMN functional connectivity across four eyes-open resting-state EEG sessions in 20 participants. Connectivity was assessed using the debiased weighted Phase Lag Index (dwPLI), a measure that reduces volume conduction effects and aims to capture non-spurious phase synchrony between electrodes. Our topographical analysis focuses on identifying stable connections across sessions, emphasizing on the alpha band due to its known relevance for resting-state activity and potential in NFB training (NFT) protocols.

# II. METHODOLOGY

# A. Participants

In this work, we present results from 20 healthy adults (15 males and 5 females), aged between 20 and 39 years (M = 27.60, SD = 5.57). None of the participants had been diagnosed with any neurological diseases. The recruitment process and study procedures adhered to ethical standards, and the research protocol was approved by the Swedish Ethical Review Authority (reference number 2021–03121).

### B. Recordings

Each participant was recruited to participate in four distinct sessions on different days. Each session started with a block of eyes-open resting-state followed by multiple blocks of NFB training. For the scope of this study, only resting-state data were analyzed. During resting-state, participants sat in a dark room with their eyes open in front of a black computer screen. Data were recorded during 5 minutes using Pycorder (Brain Products), in-house LabVIEW (National Instruments) and MATLAB (MathWorks) as a system interface.

1) Electroencephalogram (EEG): EEG data were recorded at a sampling rate of 1 kHz using 64 active electrodes arranged as per the extended 10-20 electrode placement system (Brain Products ActiCHamp). One of the active electrodes was placed on the tip of the left nostril to serve as the reference electrode and another one was placed below the right eye to measure vertical eye movements. Our data analysis were performed on the remaining total 62 active electrodes placed on the scalp. Electrooculogram (EOG) and horizontal eye movements were also recorded using two additional passive electrodes placed 1 cm lateral to the left and right outer canthi of the eye. Impedances were maintained below 40 kOhms throughout all sessions.

### C. EEG Preprocessing Pipeline

EEG data were preprocessed using MATLAB R2024a and the EEGLAB toolbox (version 2024.2.1) [21]. The following steps were applied on raw EEG data: (1) Power line noise artifacts were removed using *pop\_cleanline* to directly attenuate 50 Hz power line interference and its second harmonic (100 Hz). A sliding window approach with spectral estimation was applied across all EEG channels. (2) Downsampling the EEG data from 1000 Hz to 100 Hz using *pop\_resample* to speed up next steps (3) A bandpass filter between 1 and 40 Hz was applied (*pop\_eegfiltnew*) with a Hamming-windowed sinc

FIR filter. This step removes slow drifts (e.g., due to movement) and high-frequency noise. (4) Data was re-referenced to the common average of all electrodes using pop\_reref. (5) Dimensionality reduction was performed with principal component analysis (PCA) to determine the number of significant components. Only components with eigenvalues greater than 1e-7 were retained. (6) Independent Component Analysis (ICA) was applied on filtered data using pop runica with the picard algorithm and PCA-based dimensionality reduction and concatenation of conditions enabled. (7) Eye-related components were automatically identified using pop\_iclabel and flagged with pop icflag if the probability of classification as 'Eye' exceeded 0.8. (8) The flagged eye-related ICA components were removed from the original EEG data (sampled at 1000Hz and band-pass filtered to 1-40Hz) using pop\_subcomp. ICA weights computed on the downsampled data were applied to the full-resolution dataset for improved temporal precision. (9) Artifact subspace reconstruction (ASR) was applied to further suppress transient, high-amplitude artifacts, using *pop\_clean\_rawdata* with the following parameters: FlatlineCriterion = 40, ChannelCriterion = -1, BurstCriterion = 4, WindowCriterion = 20, BurstRejection = 'off', Highpass = 'off', and Distance = 'Euclidian'. Importantly, BurstRejection = 'off' does not reject entire data windows but instead applies artifact suppression to individual bursts. If any bad channels were detected (via clean channel mask), spherical spline interpolation was performed using pop interp. (10) A surface Laplacian filter was finally applied [22], implemented as laplacian perrinX, with a smoothing parameter of 1e-5. This step enhanced spatial resolution by attenuating volume conduction effects.

# D. Data Analyses

EEG data were transformed into the time-frequency domain using complex Morlet wavelets across a frequency range of 1–40 Hz. The wavelets were defined with frequency-dependent full-width at half-maximum (FWHM) values as in [23]. This yielded a complex-valued time-frequency representation of the signal for each electrode, frequency, and time point. The resulting signal was downsampled by a factor of 10 and used for subsequent phase-lag index (PLI) computations.

For this study, from the complex signal we extracted the alpha frequencies (8–12 Hz). The averaged signal across these frequencies was decomposed in non-overlapping 20-second windows, and debiased weighted phase-lag index (dwPLI) matrices were calculated for all windows (approx 15 windows for 5 minutes) and electrodes.

1) Debiased Weighted Phase Lag Index (dwPLI): The phase-lag index (PLI) is a measure of phase synchronization between two signals and was used as the fundamental method to estimate EEG functional connectivity during rest using 62 electrodes (1891 unique electrode pairs). PLI-based measures are known to be well suited for resting-state activity or tasks in which connectivity strength is not compared across conditions because they minimize volume conduction contamination [24], which would otherwise obscure true connectivity patterns

when comparing conditions. To improve upon the original PLI we employed the debiased weighted (dw) PLI, which assigns more weight to phase differences further from zero, thereby reducing the influence of near-zero-lag connections (often associated with volume conduction or common sources), and corrects for the bias introduced by small sample sizes [25]. We adapted the dwPLI implementation [24] to match our dataset structure, and trials were created by splitting the data into windows.

### E. Validation of Connectivity Results Using Surrogate Data

To identify statistically significant connections, we generated null distributions of dwPLI values through a surrogate data approach:

1) Surrogate Generation: For each session (4 sessions per subject), we generated 1000 surrogate datasets by disrupting the phase relationship between electrode pairs. This was done by circularly shifting (circshift) the time series of one electrode in each pair by a random number of samples (in the range [10, N–10], where N is the signal length), preserving spectral properties while pseudo-randomizing genuine phase synchrony.

For each surrogate iteration, dwPLI was computed across all time windows, and the values were averaged to obtain one surrogate dwPLI per electrode pair. This resulted in 1000 surrogate-based dwPLI values per electrode pair, forming a null distribution. The observed/real dwPLI values (averaged across windows) were then compared to their corresponding null distributions. A p-value was computed for each electrode pair by calculating the proportion of surrogate values that were equal to or greater than the observed dwPLI. Electrode pairs with p-values below 0.05 were considered statistically significant. Only these connections were retained for further analysis.

The coefficient of variation (CV) was calculated for each of these significant connections across the  $\sim 15$  time windows to assess the temporal stability of functional connectivity within a single session. To exclude unstable and transient connections, we selected the 30% of connections with the lowest CV values, here referred to as stable connections. We tested different thresholds within a range of 10-30%, however 30% allowed for a good compromise between stability and sample size. The use of a proportional threshold is supported by previous findings showing that it produces more stable network measures, particularly for fMRI eyes-open resting-state recordings [26]. There is a lack of consensus on the ideal threshold for wholebrain network analyses and an arbitrary threshold or range of thresholds is typically used [26]. Choosing a more conservative threshold (e.g., the lowest 10%) would restrict the analysis to only the most temporally stable connections, thereby reducing noise but potentially excluding other meaningful connections that exhibit slightly higher variability. Given the limited spatial resolution of scalp EEG, particularly its inability to reliably capture signals from deep subcortical regions such as the hippocampus, it remains challenging to comprehensively assess the long-term stability of DMN connectivity regions. For this

reason, we adopted a more inclusive 30% threshold, allowing us to to capture a broader range of potentially significant interactions, but at the risk of incorporating less stable ones. This approach is supported by evidence that, despite short-term fluctuations, stable functional networks can emerge over longer EEG recordings [7], highlighting the value of using less conservative thresholds to uncover persistent network structures over time.

A false discovery rate (FDR) step was applied to correct for multiple comparisons [27] and control for type I errors among our stable connections.

### F. Defining DMN ROIs

We selected the alpha frequency band (8-12Hz) for analysis due to its prominence in resting-state EEG recordings [15], [28], [29] [14] as well as the stronger positive correlation between DMN and the alpha rhythm [30].

We further approximated DMN regions [3] (e.g., medial prefrontal cortex, posterior cingulate cortex, inferior parietal lobes) to our extended 10-20 EEG electrodes locations by evaluating a graphic representation of Montreal Neurological Institute (MNI) coordinates of DMN anatomical regions [28] and DMN seeds [31], operational modules [19] and montage of DMN-related EEG channels previously described [32]. We defined 4 Regions of interest (ROIs): Frontal (F), Left-Parietal (LP), Right-Parietal (RP) and Medial (M) (see Tab. I), generating a total of 6 possible connections within the DMN: LPM (Left-Parietal-Medial), LPRP (Left-Parietal-Right-Parietal), LPF (Left-Parietal-Frontal), MRP (Medial-Right-Parietal), MF (Medial-Frontal), RPF (Right-Parietal-Frontal). We then averaged dwPLI and subject count per connection within these ROIs, focusing our analysis in ROIto-ROI connectivity. Only connections that were significant, belonged to the 30% lowest CVs, and survived the FDR step were considered, and ROIs were displayed only if they had at least one significant connection with another ROI.

TABLE I Regions of Interest (ROIs) and corresponding EEG electrodes

ROI label	Electrodes
Frontal (F)	'Fp1', 'Fp2', 'AF3', 'AFz', 'AF4', 'F3', 'F1', 'Fz', 'F2', 'F4'
Left-Parietal (LP)	'CP5', 'CP3', 'P1', 'P3', 'P5', 'P7', 'P03', 'P07'
Right-Parietal (RP)	'CP4', 'CP6', 'P2', 'P4', 'P6', 'P8', 'P04', 'P08'
Medial (M)	'CPz', 'Pz', 'POz'

### III. RESULTS

The overall averaged dwPLI for significant and stable DMN connections, aggregated across four sessions and twenty subjects, is shown in Fig. 1. Notably, all twenty participants showed intra-session stability in LPF, LPRP, LPM in at least one session and posterior short-range connections show greater

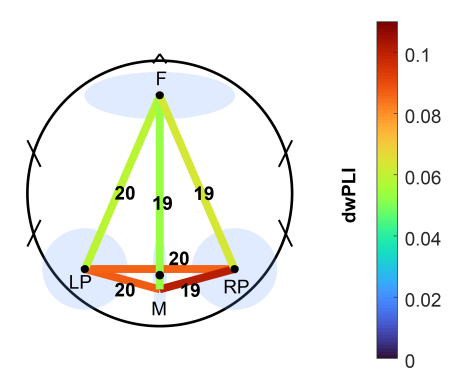


Fig. 1. Overall functional connectivity (dwPLI) across all sessions. Each line represents a functional connection between ROIs, with the color indicating the mean dwPLI value and the number displaying how many participants (out of 20) exhibited intra-session stability in that connection.

dwPLI values. First, we analyzed the averaged dwPLI of our intra-session stable connections for each resting-state session and each ROI following the previously outlined methods outlined.

To complement Fig.1, we provide a breakdown of connection stability across sessions in Fig.2. Each subfigure represents the number of participants whose functional connection between two ROIs was exclusively stable in a specific number of sessions: connections stable in (a) only one session, (b) exactly two sessions, (c) exactly three sessions, and (d) in all four sessions. The numbers on each line indicate the number of participants meeting the stability criterion for that connection, while the line color reflects the mean dwPLI across those participants and connections. Moreover, in Fig. 2(d), we can see that 16 out of 20 participants had a stable LPRP connection across all four sessions, suggesting high intersession consistency in that DMN pathway. Furthermore, it is noticeable that short-range connections exhibit greater stability when compared to long-range ones.

Furthermore, none of the participants showed complete

instability of DMN connectivity, having at least two connections, independently of which specific ones, that remained stable across three out of four resting-state sessions. Moreover, the majority of subjects demonstrated a high degree of consistency, with five out of six DMN connections remaining stable in at least three sessions. These patterns of intra-session stability are illustrated in Fig. 3.

# IV. DISCUSSION

In this work, we focus only on EEG data because, to the best of our knowledge, no EEG studies have examined the stability of DMN connectivity across multiple resting-state sessions in healthy participants. In fMRI literature, some studies have investigated test-retest reliability of resting-state networks, including the DMN, but rarely specifying which connections within the DMN remain stable and in how many individuals over repeated sessions [33], [34].

Our results fill this gap by quantifying the consistency of DMN connectivity patterns across four EEG resting-state sessions, as shown in Fig. 2. This approach allows us to identify both which DMN pathways are most consistently preserved and the number of subjects in which such stability occurs.

These DMN regions are known to be involved in self-reflection and internally focused thoughts [3]. The fact that they stay strongly connected across sessions suggests they might form a kind of "core" subnet within the DMN, at least in the alpha band. Specifically, the consistent presence of stable connections in these regions might indicate that they could be functionally relevant. Such stable connectivity patterns might be a valuable feature to integrate into EEG-based BCI systems, where having consistent brain signals is key for accurate neural decoding and neurofeedback applications.

Our findings show that DMN connections exhibit a high degree of stability across multiple EEG resting-state sessions in most participants (Fig. 1). In particular, none of the participants had zero stable connections in three sessions (Fig. 3) which suggests a robust structure of the DMN. Furthermore, the stability of DMN connectivity across time has also been

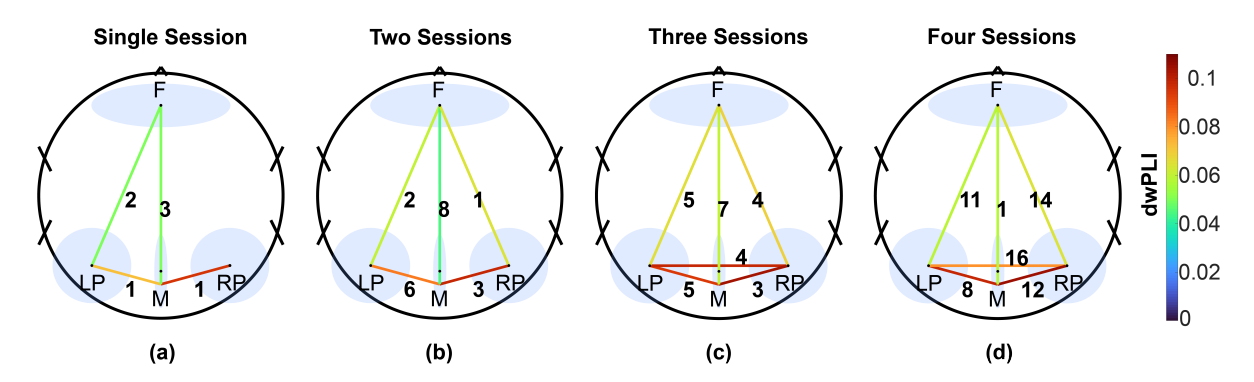


Fig. 2. Session-specific stability of DMN connections. The color indicates the average dwPLI for each connection, and the number shows the count of participants with a intra-session stable connection in (a) only one session, (b) two sessions, (c) three sessions, or (d) all four sessions.

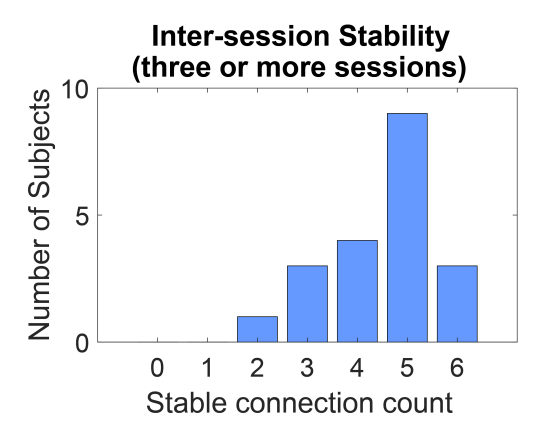


Fig. 3. Histogram of Subjects with a given number of intra-session stable connections across at least 3 out of 4 sessions. Each subject could have all 6 connections stable (LPM, LPRP, LPF, MRP, MF, RPF), none, or just a few.

linked to healthy brain function [6] and could be used as a biomarker to predict who will succeed or fail at self-regulation. The DMN could also be used as an independent biomarker during neurofeedback to measure task compliance and evaluate if the participants are actively trying to regulate their brain activity. In other words, if the DMN becomes active during easy tasks because people start mind-wandering, then the change in its activity between practiced and new tasks should be linked to how much a person tends to mind-wander [2].

In the context of neurofeedback training, especially for BCI applications, DMN metrics could potentially be used to characterize individual mental states during rest or training [35]. Our results reveal inter-subject variability in the number and configuration of stable connections (as shown in Fig. 3) across sessions. Such variability may reflect differences in internal thought processes, attention regulation and learning strategies [35], or even individual susceptibility to mindwandering. This inter-subject variability might be a concern if we want to generalize our results and link DMN stability to NFT performance, which could be addressed by using a larger sample size.

Notably, our topographical analysis revealed that connections along the occipital-parietal exhibited stronger phase synchronization, as reflected by higher dwPLI values. On the other hand, longer-range connections were weaker. This spatial pattern of stability and connectivity strength suggests that posterior medial regions of the DMN are particularly stable and synchronously active during resting-state EEG. Interestingly, the medial parietal DMN regions (PCC/precuneus) have shown enhanced alpha-band effective connectivity in patients with social anxiety disorder [20], pointing to the potential clinical relevance of these DMN sub-regions. Furthermore, a previous study demonstrated that stronger resting-state functional connectivity between the medial frontal cortex and PCC (key nodes of the DMN) was associated with better working memory performance [36], highlighting a link between DMN and cognitive performance. Extending this, a recent study [35] showed that individual and design-specific factors significantly

influenced neurofeedback performance, reinforcing the role of intrinsic brain network variability in BCI outcomes.

Although many previous studies have explored the stability of DMN using fMRI [35], [36], our findings demonstrate that EEG can offer a practical and low-cost alternative for tracking the dynamics of DMN connectivity over time. Additionally, unlike most resting-state EEG studies that focus on eyesclosed conditions, our work contributes to the understanding of DMN dynamics under an eyes-open protocol, which better reflect the natural setting of BCI training.

Previous research has linked fMRI-based resting-state networks with specific EEG frequency bands during eyes-closed rest, particularly showing stronger positive correlation between alpha rhythm and DMN [30]. Our work adds value to the field by using eyes-open recordings and suggesting that alpha-band connectivity metrics may serve as useful indicators of network stability.

We used functional connectivity measures to estimate intrasession dwPLI stability within the DMN and whether or not those connections were replicated across sessions and subjects. Our topographical analysis shows where connectivity changes occur on the scalp and how they evolve over time in the alpha band. Future work should evaluate the strength and stability of connectivity across different frequency bands. Additionally, metrics such as graph theory and clustering coefficients could be applied to better understand the network structure.

Most importantly, it is worth noting that our network structure stability relied on a threshold of 30% of the lowest CV in all significant connections, and different thresholds could lead to different results, particularly for fMRI eyes-open resting-state recordings [26]. On another note, eyes-open might produce more "non-specific brain activation" than closed eyes condition, leading to more variability and less stability in the connectivity patterns [37]. Furthermore, gender imbalances and applying different thresholds between sex groups might have also led to different outcomes [26], [38]. This is one of the main challenges in the functional connectivity thresholding problem, as there is no "ground truth" method on how to define the best threshold value [38].

# V. CONCLUSION

This study shows that EEG-based functional connectivity within the Default Mode Network remained relatively stable across multiple eyes-open resting-state sessions in a group of healthy participants. By identifying consistent alpha-band connectivity patterns across sessions and participants, the results suggest that individual brain network characteristics can be reliably measured. These findings also encourage further investigation into how DMN connectivity relates to other frequency bands, cognitive traits, training outcomes, and network topology.

### ACKNOWLEDGMENT

This work was supported by the Knowledge Foundation KKS HÖG grant (project number 20190099), Åke Wibergs

foundation (project number M21-0043), Eskilstuna municipality through the project Sörmlandskontraktet, and Mälardalen University.

# REFERENCES

- R. L. Buckner, J. R. Andrews-Hanna, and D. L. Schacter, "The brain's default network: anatomy, function, and relevance to disease," *Annals of the new York Academy of Sciences*, vol. 1124, no. 1, pp. 1–38, 2008.
- [2] M. F. Mason, M. I. Norton, J. D. Van Horn, D. M. Wegner, S. T. Grafton, and C. N. Macrae, "Wandering minds: the default network and stimulus-independent thought," *science*, vol. 315, no. 5810, pp. 393–395, 2007.
- [3] M. E. Raichle, "The brain's default mode network," Annual review of neuroscience, vol. 38, no. 1, pp. 433–447, 2015.
- [4] V. Menon, "20 years of the default mode network: A review and synthesis," *Neuron*, vol. 111, no. 16, pp. 2469–2487, Aug. 2023.
- [5] N. Cooray, C. Gohil, B. Harris, S. Frost, and C. Higgins, "Default Mode Network Detection using EEG in Real-time," Apr. 2024, iSSN: 2430-5235 Pages: 2024.04.03.24305235.
- [6] L. Beason-Held, M. Kraut, and S. Resnick, "Stability Of Default-Mode Network Activity In The Aging Brain," *Brain imaging and behavior*, vol. 3, no. 2, pp. 123–131, Jan. 2009.
- [7] C. J. Chu, M. A. Kramer, J. Pathmanathan, M. T. Bianchi, M. B. Westover, L. Wizon, and S. S. Cash, "Emergence of stable functional networks in long-term human electroencephalography," *Journal of Neuroscience*, vol. 32, no. 8, pp. 2703–2713, 2012.
- [8] G. Goelman, R. Dan, O. Bezdicek, R. Jech, and D. Ekstein, "Directed functional connectivity of the default-mode-network of young and older healthy subjects," *Scientific Reports*, vol. 14, no. 1, p. 4304, Feb. 2024, publisher: Nature Publishing Group.
- [9] B. Blankertz, C. Sannelli, S. Halder, E. M. Hammer, A. Kübler, K.-R. Müller, G. Curio, and T. Dickhaus, "Neurophysiological predictor of smr-based bci performance," *Neuroimage*, vol. 51, no. 4, pp. 1303–1309, 2010
- [10] J. Reis, A. M. Portugal, L. Fernandes, N. Afonso, M. Pereira, N. Sousa, and N. S. Dias, "An alpha and theta intensive and short neurofeedback protocol for healthy aging working-memory training," *Frontiers in Aging Neuroscience*, vol. 8, 2016.
- [11] S. Enriquez-Geppert, R. J. Huster, and C. S. Herrmann, "EEG-Neurofeedback as a Tool to Modulate Cognition and Behavior: A Review Tutorial," *Front. Hum. Neurosci.*, vol. 11, Feb. 2017, publisher: Frontiers.
- [12] B. Allison, T. Luth, D. Valbuena, A. Teymourian, I. Volosyak, and A. Graser, "BCI demographics: How many (and what kinds of) people can use an SSVEP BCI?" *IEEE transactions on neural systems and rehabilitation engineering*, vol. 18, no. 2, pp. 107–116, 2010.
- [13] O. Alkoby, A. Abu-Rmileh, O. Shriki, and D. Todder, "Can we predict who will respond to neurofeedback? a review of the inefficacy problem and existing predictors for successful EEG neurofeedback learning," *Neuroscience*, vol. 378, pp. 155–164, 2018.
- [14] A. Berkovich-Ohana, J. Glicksohn, and A. Goldstein, "Studying the default mode and its mindfulness-induced changes using EEG functional connectivity," *Social Cognitive and Affective Neuroscience*, vol. 9, no. 10, pp. 1616–1624, Oct. 2014.
- [15] K. Jann, M. Kottlow, T. Dierks, C. Boesch, and T. Koenig, "Topographic Electrophysiological Signatures of fMRI Resting State Networks," *PLOS ONE*, vol. 5, no. 9, p. e12945, Sep. 2010, publisher: Public Library of Science.
- [16] J. Samogin, Q. Liu, M. Marino, N. Wenderoth, and D. Mantini, "Shared and connection-specific intrinsic interactions in the default mode network," *Neuroimage*, vol. 200, pp. 474–481, 2019.
- [17] A. Das, C. de Los Angeles, and V. Menon, "Electrophysiological foundations of the human default-mode network revealed by intracranialeeg recordings during resting-state and cognition," *Neuroimage*, vol. 250, p. 118927, 2022.
- [18] M. Marino, G. Arcara, C. Porcaro, and D. Mantini, "Hemodynamic correlates of electrophysiological activity in the default mode network," *Frontiers in Neuroscience*, vol. 13, p. 1060, 2019.
- [19] A. A. Fingelkurts, A. A. Fingelkurts, S. Bagnato, C. Boccagni, and G. Galardi, "The chief role of frontal operational module of the brain default mode network in the potential recovery of consciousness from the vegetative state: a preliminary comparison of three case reports," *The Open Neuroimaging Journal*, vol. 10, p. 41, 2016.

- [20] A. Al-Ezzi, N. Kamel, I. Faye, and E. Gunaseli, "Analysis of Default Mode Network in Social Anxiety Disorder: EEG Resting-State Effective Connectivity Study," *Sensors*, vol. 21, no. 12, p. 4098, Jan. 2021, number: 12 Publisher: Multidisciplinary Digital Publishing Institute.
- [21] A. Delorme and S. Makeig, "Eeglab: an open source toolbox for analysis of single-trial eeg dynamics including independent component analysis," *Journal of neuroscience methods*, vol. 134, no. 1, pp. 9–21, 2004.
- [22] F. Perrin, J. Pernier, O. Bertrand, and J. F. Echallier, "Spherical splines for scalp potential and current density mapping," *Electroencephalogra*phy and clinical neurophysiology, vol. 72, no. 2, pp. 184–187, 1989.
- [23] M. X. Cohen, "A better way to define and describe morlet wavelets for time-frequency analysis," *NeuroImage*, vol. 199, pp. 81–86, 2019.
- [24] —, Analyzing neural time series data: theory and practice. MIT press, 2014.
- [25] M. Vinck, R. Oostenveld, M. van Wingerden, F. Battaglia, and C. M. A. Pennartz, "An improved index of phase-synchronization for electrophysiological data in the presence of volume-conduction, noise and sample-size bias," *NeuroImage*, vol. 55, no. 4, pp. 1548–1565, Apr. 2011.
- [26] K. A. Garrison, D. Scheinost, E. S. Finn, X. Shen, and R. T. Constable, "The (in) stability of functional brain network measures across thresholds," *Neuroimage*, vol. 118, pp. 651–661, 2015.
- [27] C. R. Genovese, N. A. Lazar, and T. Nichols, "Thresholding of statistical maps in functional neuroimaging using the false discovery rate," *Neuroimage*, vol. 15, no. 4, pp. 870–878, 2002.
- [28] A. Al-Ezzi, N. Kamel, I. Faye, and E. Gunaseli, "Analysis of default mode network in social anxiety disorder: Eeg resting-state effective connectivity study," *Sensors*, vol. 21, no. 12, p. 4098, 2021.
- [29] G. G. Knyazev, J. Y. Slobodskoj-Plusnin, A. V. Bocharov, and L. V. Pylkova, "The default mode network and eeg alpha oscillations: an independent component analysis," *Brain research*, vol. 1402, pp. 67–79, 2011.
- [30] D. Mantini, M. G. Perrucci, C. Del Gratta, G. L. Romani, and M. Corbetta, "Electrophysiological signatures of resting state networks in the human brain," *Proceedings of the National Academy of Sciences of the United States of America*, vol. 104, no. 32, pp. 13170–13175, Aug. 2007
- [31] F. Fusina, M. Marino, C. Spironelli, and A. Angrilli, "Ventral attention network correlates with high traits of emotion dysregulation in community women—a resting-state eeg study," Frontiers in Human Neuroscience, vol. 16, p. 895034, 2022.
- [32] M. Rusiniak, A. Wróbel, K. Cieśla, A. Pluta, M. Lewandowska, J. Wójcik, P. Skarżyński, and T. Wolak, "The relationship between alpha burst activity and the default mode network," *Acta Neurobiologiae Experimentalis*, vol. 78, no. 2, pp. 92–113, 2018.
- [33] Z. Shehzad, A. C. Kelly, P. T. Reiss, D. G. Gee, K. Gotimer, L. Q. Uddin, S. H. Lee, D. S. Margulies, A. K. Roy, B. B. Biswal *et al.*, "The resting brain: unconstrained yet reliable," *Cerebral cortex*, vol. 19, no. 10, pp. 2209–2229, 2009.
- [34] X.-N. Zuo, A. Di Martino, C. Kelly, Z. E. Shehzad, D. G. Gee, D. F. Klein, F. X. Castellanos, B. B. Biswal, and M. P. Milham, "The oscillating brain: Complex and reliable," *NeuroImage*, vol. 49, no. 2, pp. 1432–1445, Jan. 2010.
- [35] A. Haugg, F. M. Renz, A. A. Nicholson, C. Lor, S. J. Götzendorfer, R. Sladky, S. Skouras, A. McDonald, C. Craddock, L. Hellrung et al., "Predictors of real-time fmri neurofeedback performance and improvement—a machine learning mega-analysis," *Neuroimage*, vol. 237, p. 118207, 2021.
- [36] M. Hampson, N. R. Driesen, P. Skudlarski, J. C. Gore, and R. T. Constable, "Brain connectivity related to working memory performance," *Journal of Neuroscience*, vol. 26, no. 51, pp. 13338–13343, 2006.
- [37] A. A. Fingelkurts, A. A. Fingelkurts, V. A. Ermolaev, and A. Y. Kaplan, "Stability, reliability and consistency of the compositions of brain oscillations," *International Journal of Psychophysiology*, vol. 59, no. 2, pp. 116–126, 2006.
- [38] T. Adamovich, I. Zakharov, A. Tabueva, and S. Malykh, "The thresholding problem and variability in the EEG graph network parameters," *Scientific Reports*, vol. 12, no. 1, p. 18659, Nov. 2022, publisher: Nature Publishing Group.